Heliyon

Coordination of early cellular reactions during activation of bone resorption in the rat mandible periosteum: An immunohistochemical study

Bassam Hassan [a,1], Isabelle Fouilloux [a,c,1], Brigitte Baroukh [a], Annie Llorens [a], Martin Biosse Duplan [b,c], Marjolaine Gosset [a,c], Marc Cherruau [a,c], Jean-Louis Saffar [a,*]

[a] EA2496 Laboratoire Pathologies, Imagerie et Biothérapies oro-faciales, Faculté de Chirurgie Dentaire, Université Paris Descartes, Sorbonne Paris Cité, Montrouge, France

[b] INSERM U1163, Institut Imagine, Université Paris Descartes, Sorbonne Paris Cité, Hôpital Necker-Enfants Malades Paris, France

[c] Assistance Publique − Hôpitaux de Paris, Paris, France

* Corresponding author.

E-mail address: jean-louis.saffar@parisdescartes.fr (J.-L. Saffar).

[1] These authors contributed equally to this work.

Abstract

The activation step of bone remodeling remains poorly characterized. Activation comprises determination of the site to be remodeled, osteoclast precursor recruitment, their migration to the site of remodeling, and differentiation. These actions involve different compartments and cell types. The aim of this study was to investigate events and cell types involved during activation. We used a bone remodeling model in rats where extractions of the upper jaw molars initiate remodeling of the antagonist lower jaw (mandible) cortex along the periosteum. In this model osteoclastic resorption peaks 4 days after extractions. We previously reported that mast cell activation in the periosteum fibrous compartment is an early event of activation, associated with recruitment of circulating monocyte osteoclast precursors. By using immunohistochemistry, we observed 9 hours after induction a

spatially oriented expression of InterCellular Adhesion Molecule-1 in the vessels that was inhibited by antagonists of histamine receptors 1 and 2. It was followed at 12 hours by the recruitment of ED1+ monocytes. In parallel, at 9 hours, Vascular Cellular Adhesion Molecule-1+ fibroblast-like cells scattered in the fibrous compartment of the periosteum between the vessels and the osteogenic compartment increased; these cells may be implicated in osteoclast precursor migration. Receptor Activator of NF KappaB Ligand+ cells increased at 12 hours in the osteogenic compartment and reached a peak at 18 hours. At 24 hours the numbers of osteogenic cells and subjacent osteocytes expressing semaphorin 3a, a repulsive for osteoclast precursors, decreased before returning to baseline at 48 hours. These data show that during activation the two periosteum compartments and several cell types are coordinated to recruit and guide osteoclast precursors towards the bone surface.

Keywords: Biological sciences, Cell biology, Physiology, Dentistry

1. Introduction

Bone remodeling involves a coordinated and highly regulated sequence of events that include activation, resorption, reversal and formation [1, 2]. In contrast with resorption and formation, which are well characterized and whose kinetics has been extensively studied at the cellular and molecular levels [3, 4, 5], activation, the step that initiates remodeling remains poorly characterized. Activation comprises the emission of local signals at the site that will undergo remodeling, recruitment of circulating osteoclast precursors, migration of the precursors toward the bone surface, and their differentiation in preosteoclasts and osteoclasts [6]. These events imply that different but spatially related compartments are involved in activation.

The signals that initiate activation emanate from the osteoblast lineage (osteogenic cells and osteocytes) that expresses pro-resorbing factors [7, 8]. The main roles of these signals, among which Receptor Activator of NF KappaB Ligand (RANKL) has a central role, are to recruit circulating osteoclast precursors and induce their differentiation into osteoclasts. Precursors adhere to activated endothelial cells, cross the endothelium and migrate toward the osteogenic cells [9, 10]. Activated endothelial cells express *in vitro* InterCellular Adhesion Molecule-1 (ICAM-1) [9, 11] to allow adhesion of osteoclast precursors to the vascular wall and migration through the vessel wall [12, 13].

In a model of alveolar bone periosteum remodeling in rats, the extractions of the upper jaw molars induce the extrusion of the lower (mandible) molars due to the loss of mechanical stimulation of these teeth. It triggers bone remodeling along the mandible cortex at the top of the alveolar crest [14]. Physiologically, this bone surface is subjected to bone formation. Nine hours after induction (i.e., extractions

of the upper molars) mast cells (MC) located in the outer fibrous layer of the periosteum (referred to here as the non-osteogenic compartment), close to a vascular network and sensory nerve fibers, are activated for a short time (their basal condition is restored at 24 h) [15]. MC activation is rapidly followed by the migration in the compartment of circulating monocytes expressing the ED1 marker and polymorphonuclear leukocytes (PMNL) [16]. Monocyte recruitment reaches a maximum at 12 hours [15, 16]. These cells go towards the bone surface after penetrating the periosteum cambium layer (referred to here as the osteogenic compartment). The osteogenic compartment, about 65 μm thick, functions as the canopy described over the endosteal envelop [17] and is constituted by mesenchymal progenitors, osteoprogenitors and secreting osteoblasts [18]. Osteoclast precursors differentiate in tartrate-resistant acid phosphatase+ pre-osteoclasts only in the osteogenic compartment [16]. Osteoclastic resorption peaks 4 days after induction.

The role of histamine released by MC is emphasized by the use of histamine receptor antagonists that drastically reduces ED1+ cell recruitment at 12 h and osteoclast numbers 4 days later [15, 19]. Histamine induces vasodilation, increased vascular permeability, expression of adhesion molecules by endothelial cells and infiltration of inflammatory cells [20, 21].

Altogether, these data raise some questions: how do periosteal vessels react following MC activation? How are the precursors guided to the bone surface? How and when do osteogenic cells and osteocytes participate to activation events? The objective of this *in vivo* immunohistochemical study was to identify cellular changes taking place in the periosteum to favor bone resorption. To this aim, we used a set of markers possibly involved in the trafficking of the osteoclast precursors to the bone surface, including (1) InterCellular Adhesion Molecule-1 (ICAM-1) to evaluate vessel reactions, (2) Vascular Cellular Adhesion Molecule-1 (VCAM-1), a modulator of monocyte and macrophage trafficking [22, 23] implicated in the early stages of osteoclast differentiation [24], (3) RANKL, and (4) semaphorin 3a (sema3a), a repulsive for preosteoclasts and osteoclasts expressed by the osteogenic cells and the osteocytes [25].

2. Material and methods

2.1. Ethics statement

This study was approved by the Animal Experimentation Ethics committee of Université Paris Descartes (approval number CEEA34.MG.036.12) and complied with European Union recommendations on laboratory animal care (EU directive 2010/63/EU). The animals were maintained in a temperature-controlled (25 °C) facility with a 12 h light/dark cycle. Prior to tooth extraction and killing, rats were anesthetized with xylazine (100 mg/kg b.w.) and ketamine (80 mg/kg b.w.) (both

from Centravet, Maisons Alfort, France). After extraction the rats were intraperitoneally injected with buprenorphine (0.02 mg/kg b.w.) to control post-operative pain.

2.2. Experimental design

A total of 138 eight weeks old male Wistar rats (Iffa Credo, L'Arbresle, France) weighing 200 ± 20 g rats were used. They were fed a standard diet for rodents (M25 Extralabo; U.A.R., Villemoisson, France); food and water were given *ad libitum*.

2.2.1. Time-course study

One hundred twenty rats were used in this study. Twenty rats were used as baseline controls. The right maxilla (upper jaw) molars of the remaining animals were extracted. Groups of 20 rats were constituted at random to be killed 9, 12 18, 24 and 48 hours after extractions.

2.2.2. Histamine receptors antagonism

Eighteen rats had their right maxillary molars extracted as previously. They were treated systemically (6 per treatment) with intramuscular injection of saline histamine receptor 1 (H1R) antagonist mepyramine solution (1.5 mg/kg/day), saline H2R antagonist famotidine solution (10 mg/kg/day;) or normal saline, beginning immediately after extractions (both from Sigma-Aldrich Corp, Lyon, France). These rats were killed 12 hours after induction, i.e. when monocyte recruitment reach a maximum.

2.3. Sample processing

The animals were killed by cardiac exsanguination. The right hemi-mandibles were dissected out and fixed in either cold (4 °C) 70% ethanol (10 animals at each time point) or 4% paraformaldehyde (10 animals at each time point). Samples from rats treated with famotidine or mepyramine were fixed in paraformaldhehyde. After washes in phosphate buffer, the bones were dehydrated in ethanol, immersed in xylene (Sigma) and embedded without demineralization in methylmethacrylate (Merck, Darmstadt, Germany) under vacuum. Polymerization was performed at −20 °C for 48 h. Four micron-thick sections were cut in the horizontal plane (i.e. perpendicular to the molar root axis) using a Polycut E microtome (Leica, Wetzlar, Germany). Three series of 8 sections were taken at the top of the crest of the alveolar process on a total height of about 100 μm where the resorption occurs [14]. Before processing, the resin was dissolved in 2-methoxyethyl acetate (Carlo Erba, Radano, Italy). The sections were sequentially stained with toluidine blue (pH 3.8), or processed for enzymochemistry of alkaline phosphatase (ALP), or for

immunohistochemistry. Toluidine blue was used for morphological observations. The 5th section of each series was processed for ALP by incubating the sections with naphthol ASTR phosphate and fast blue RR (pH 9) to reveal osteogenic cells (preosteoblasts and osteoblasts). Each marker staining was assigned a position within the series on either side of the ALP-stained section, so that two sections stained for a marker were 32 µm apart.

2.4. Immunohistochemistry

Mouse monoclonal antibodies against HIS48 (ref 554905, BD Biosciences Pharmingen, San Diego, CA, USA: 1:100), ED1 (murine equivalent of CD68, MAB1435, Chemicon, Temecula, CA, USA; 1:100), CD54 (ICAM-1, ref 554967, BD Biosciences Pharmingen, 1:50) and rabbit polyclonal antibodies against CD106 (VCAM-1, SC-8304, Santa Cruz Biotechnology, Santa Cruz, CA, USA; 1:50), RANKL (ref 3963, ProSci, Poway, CA, USA; 1/160), semaphorin 3a (ab23393, Abcam, Cambridge, UK; 1:50), laminin (L9393, Sigma; 1:25) were used. Ten percent normal horse serum (Eurobio, Les Ulis, France) (monoclonal antibody), normal goat or rabbit sera (Eurobio) (polyclonal antibodies) in 0.1 M PBS with 0.05% Tween 20 were used to reduce nonspecific background. The sections were incubated overnight with primary antibodies and then with the relevant secondary biotinylated antibody (Vector, Burlingame, CA, USA) with 3% hydrogen peroxide and an avidin-biotin peroxidase complex (ABC Vectastain kit, Vector). Diaminobenzidine tetrahydrochloride (Sigma) was the chromogen. Negative controls were prepared by omitting the primary antibody, by replacing the primary antibody with nonimmune serum at the same dilution, or by using an irrelevant secondary antibody. Depending on the antibody used, the reaction was processed on samples fixed with either ethanol or paraformaldehyde.

Double immunostaining was used to identify PMNL undergoing apoptosis. Sections were incubated overnight with the monoclonal antibody (HIS48), the secondary biotinylated antibody (horse anti-mouse IgG; Vector) and streptavidine FP488 (Interchim, Montluçon, France; 1:200). The sections were then incubated in the dark with polyclonal anti caspase-3 antibody (Biocarta, San Diego, CA, USA; 1:500) and with antirabbit secondary TRITC antibody (T6778, Sigma-Aldrich). Negative control procedures were used as previously.

2.5. Morphometry

The sections were examined at a constant magnification (x 260) with a semi-automatic image analyzer. The periosteal zone of interest extended along the buccal cortex from the distal face of the mesial root of the first molar to the distal face of its distal root. The ALP staining revealed a thick layer of ALP+ osteogenic cells, separated from the mineralized bone surface by a layer of osteoid tissue. The

ALP layer was used as a reference to divide the periosteum into osteogenic and non-osteogenic compartments [14]. The ALP+ layer was outlined on the computer screen and recorded. It was then superimposed on each section of the relevant series. This allowed us to visualize the location of the ALP layer in the specifically stained sections. The measurements were made on 2 sections per animal for each marker.

The following parameters were recorded in the osteogenic compartment: length of the reference bone segment, numbers of cells immunopositive for RANKL and sema3a per mm of adjacent bone surface (N/mm), number of sema $3a^+$ osteocytes in the first 60 μm from the bone surface [26].

In the non-osteogenic compartment, we quantified the number of vessel profiles (vessels per millimeter of adjacent bone surface), their mean lumen area (in $μm^2$), the numbers of $HIS48^+$ cells, ED1+ cells and VCAM-1 fibroblast-like cells (all per millimeter of adjacent bone surface).

2.6. Statistics

The data were compared (7 samples per group and per fixation technique) using nonparametric tests (Kruskal–Wallis test followed, if significant, by group comparisons with the Mann–Whitney *U*-test). Differences were considered significant at $p < 0.05$. Data are expressed as means ± SEM.

3. Results

The events occurring in the non-osteogenic compartment were studied at 0, 9, 12 and 18 h, and in the osteogenic compartment at 0, 12, 18, 24 and 48 h.

3.1. The non-osteogenic compartment

3.1.1. Vascular responses

Vessels were identified in toluidine blue-stained sections. To validate vessel identification, adjacent sections were immunostained in some samples for laminin, a marker of vessel basement membrane. We found good agreement between the two staining methods (Fig. 1).

The mean number of vessel profiles per mm of adjacent bone surface did not change. In contrast their mean caliber increased at 12 h (+ 58.5%; $p < 0.03$ vs 9 h) and returned to baseline at 18 h (- 39%; $p < 0.03$ vs 12 h) (Fig. 2a).

At baseline only a few vessels were stained positive for ICAM-1; the staining was thin and weak along the internal wall of the vessels (Fig. 2b). At 9 h and 12 h a thick immunostaining of the luminal surface of the vessel oriented towards the
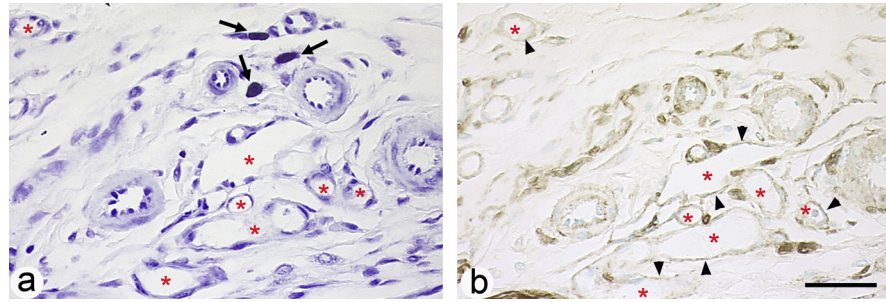
Fig. 1. Visualization of periosteum vessels in adjacent sections using two different staining techniques. **a** Toluidine blue technique. **b** Immunostaining for laminin. Asterisks show corresponding vessels with the two staining techniques. Arrows in **a** point out to mast cells. Arrowheads in **b** point out to the thin laminin staining along vessel walls. Bar = 50 μm.

bone surface was present; no staining was seen along the opposite side of these vessels (Fig. 2c). At 18 h the immunostaining returned to baseline.

The effect of mepyramine (H1R antagonist) and famotidine (H2R antagonist) were evaluated at 12 h on ICAM-1 expression. ICAM-1 was weakly expressed in the two anti HR-treated groups (Fig. 2d and e), compared with their 12 h saline-treated controls. The expression was close to that found in vessels from intact (baseline) animals.

3.1.2. Recruitment of circulating cells

At baseline 10.1 ± 1.6 ED1+ cells resided in the non-osteogenic compartment, mostly near the osteogenic compartment. They increased in the vascular environment at 12 h (+290% vs baseline, $p < 0.01$) and persisted up to 18 h (+310% vs baseline; $p < 0.03$) (Fig. 2f).

HIS48+ PMNL that were further identified by their morphology and ALP staining [27] were scarcely present at baseline (0.45 ± 0.45). They increased at 9 h (67x at 9 h vs baseline; $p < 0.0001$), reached a peak at 12 h and remained stable until 18 h (124x at 12 h vs baseline; $p < 0.005$) (Fig. 2f). Notably, PMNL morphology differed at 12 h and 18 h: the immunostaining was strong and occupied a significant part of the cells at 12 h (Fig. 2g), while it was weak and peripheral at 18 h (Fig. 2h). As PMNL are short-lived in the tissues, we assumed that they were apoptotic. Co-localization of anti-caspase 3 and anti-granulocyte antibodies confirmed that HIS48+ PMNL were apoptotic (Fig. 2i).

Elongated, fibroblast-like VCAM-1+ cells were scattered between the vessels and the osteogenic layer (Fig. 3a). They increased as soon as 9 h (2.3x; $p < 0.02$ vs baseline); they had returned to baseline at 18 h (Fig. 3b).
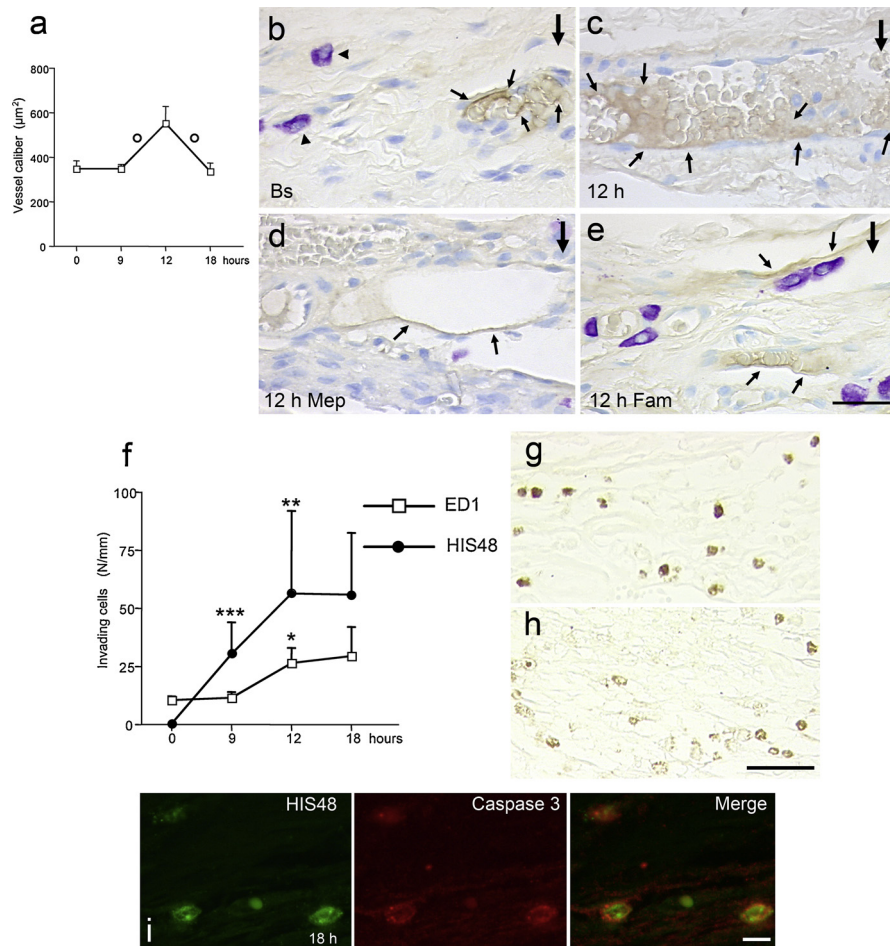
Fig. 2. Changes in the non-osteogenic compartment (= fibrous layer) of the periosteum. **a** Changes in vessel caliber. **b** to **e**: ICAM-1 expression in vessels. **b** At baseline (Bs), thin ICAM-1 immunostaining underlines the wall of some periosteal vessels (arrows). **c** At 12 h, ICAM-1 expression is thick and extends within the vessel lumen. Expression is polarized towards the bone surface. **d** ICAM-1 expression in a mepyramine (H1 receptor antagonist)-treated animal. **e** ICAM-1 expression in a famotidine (H2 receptor antagonist)-treated animal. ICAM-1 expression is minimal with the two treatments. The thick arrows in the right top corner point out towards the bone surface. The arrowheads point out to mast cells close to the vessels. Counterstaining toluidine blue. Bar = 50 μm. **f** Kinetics of HIS48+ polymorphonuclear leukocytes (PMNL) and ED1+ monocytes changes. **g** and **h** Immunostaining for HIS48+ PMNL. **g** At 12 h. **h** At 18 h. Immunopositive cells were as numerous at the two time points. While the immunostaining was strong and uniform at 12 h, it was weak and irregular in most cells at 18 h. Bar = 30 μm. **i** Double immunofluorescence for HIS48 and caspase 3 in an 18 h sample. Merging of the two images shows that HIS48+ PMNL were apoptotic at this time point. Bar = 10 μm. * p<0.01; ** p<0.005; *** p<0.0001 versus baseline. ° p<0.03 versus the preceding time point.

3.2. The osteogenic compartment

Cells of the osteogenic compartment expressed VCAM-1. At baseline, immuno-positive cells were scattered throughout the osteogenic compartment (Fig. 3c). At
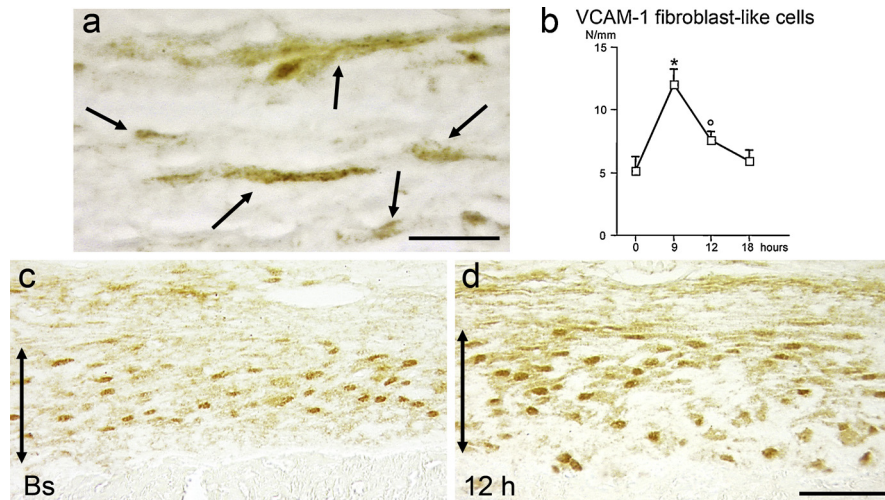
Fig. 3. VCAM-1 expression in the periosteum. **a** Immunostaining of fibroblast-like cells in the non-osteogenic compartment (arrows). Bar = 30 μm. **b** Changes with time in VCAM-1+ fibroblast-like cells. **c** and **d** Osteogenic compartment (= cambium layer). At baseline (Bs), immunopositive cells are evenly distributed within the compartment (**c**). Instead at 12 h (**d**) stained cells are preferentially located at the periphery of the compartment. Bar = 50 μm. The double arrows delineate the osteogenic compartment. * p<0.002 versus baseline °p<0.05 versus the preceding time point.

12 h the marker was preferentially expressed in cells at the periphery of the compartment (Fig. 3d).

The number of RANKL+ cells (Fig. 4a–c) was increased at 12 h (+ 40% vs baseline, p < 0.05) and reached a peak at 18 h (+ 63% vs baseline, p < 0.01). Then they significantly decreased. The immunopositive cells were located throughout the compartment. The osteocytes close to the bone surface did not express RANKL.

In the osteogenic layer, the number of sema3a+ cells strongly decreased at 24 h (-77%, p < 0.01 vs baseline); it returned to baseline at 48 h (5x, p < 0.02 vs 24 h). The decrease in sema3a+ osteocytes in a 60 μm-deep layer of bone below the bone surface was more precocious as it begun at 18 h (- 54%, p = 0.01 vs baseline), continued to decline at 24 h (-72%, p < 0.005 vs baseline) and increased at 48 h (+ 230%, p = 0.05 vs 24 h) (Fig. 4d–f).

4. Discussion

Cellular and molecular events occurring in the two compartments of the mandible periosteum were associated with circulating monocyte recruitment, their migration towards the osteogenic compartment where priming messages permitted their differentiation in the osteoclastic lineage. Coordinated signals seem to allow precursor migration to the bone surface.
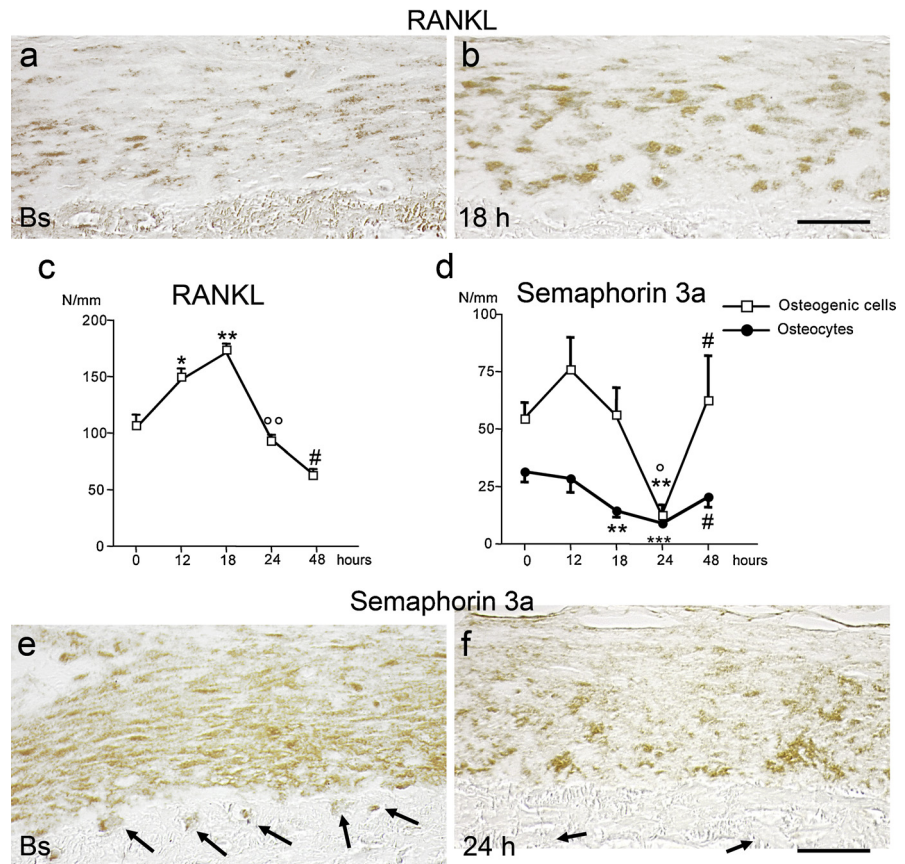
Fig. 4. Osteogenic compartment. **a** and **b**: Immunostaining for RANKL. At baseline (Bs) a few immunopositive cells are scattered within the compartment. At 18 h (**b**), RANKL+ cells were more numerous. The staining was stronger than at baseline. Bar = 50 μm. **c** Changes with time in RANKL+ cells. **d** Variations in osteogenic cells and osteocytes expressing semaphorin3a. **e** and **f** Immunostaining for semaphorin 3a. At baseline most osteogenic cells were immunopositive as were the osteocytes (arrows) subjacent to the bone surface. At 24 h, only a few cells expressed the marker while the osteocytes no longer expressed it. Bar = 50 μm. * $p \leq 0.05$; ** $p < 0.01$; *** $p < 0.005$ versus baseline. ° $p < 0.02$; °° $p < 0.003$ versus 18 h. # $p < 0.05$ versus 24 h.

As soon as 9 h after induction of the remodeling sequence, vessels strongly expressed ICAM-1, and at 12 h a transient vasodilatation occurred. ICAM-1 expression was polarized, directing the ED1+ cells towards the bone surface. Histamine up-regulates ICAM-1 expression early during inflammation [22, 23] and ICAM-1 promotes adhesion and transendothelial migration of monocyte osteoclast precursors [13]. Treating animals with H1R and H2R antagonists inhibited ICAM-1 up-regulation, resulting in a decreased ED1+ cell recruitment at 12 h, and a deficit in osteoclasts at 48 h [19].

Parfitt (1998) stated that circulating osteoclast precursors are addressed to the resorption site through an "area code" consisting of signals expressed by circulating and endothelial cells so that only osteoclast precursors are recruited

[28]. Here, not only ED1+ osteoclast precursors, but also PMNL entered the site, as they can bind ICAM-1 [29]. PMNL were apoptotic at 18 h and rapidly vanished [16]. Cell recruitment was thus not specific to osteoclast precursors.

Once in the perivascular space, ED1+ osteoclast precursors have to reach the osteogenic compartment (a distance of about 100 μm) where they differentiate into preosteoclasts. VCAM-1 expressed by fibroblast-like cells residing in the non-osteogenic compartment may guide them towards the osteogenic compartment whose cells express VCAM-1. VCAM-1 is a modulator of monocyte and macrophage trafficking [22, 30] and its induction in fibroblasts is histamine-dependent [31]. In the early stages of osteoclast differentiation, prior to RANKL signaling [32], interactions of osteoclast precursors with VCAM-1-expressing cells are critical [24]. Moreover, VCAM-1 expressed by osteogenic cells enhances osteoclast precursor penetration in the site of bone remodeling [32]. Although we did not observe an increase in VCAM-1+ cells in the osteogenic compartment, a redistribution of the marker occurred: at 12 h VCAM-1 was preferentially expressed in cells at the periphery of the compartment. This may allow the trafficking of the osteoclast precursors from a compartment to the other.

RANKL was constitutively expressed throughout the osteogenic compartment, as it is essential to the survival of the few preosteoclasts present [16]. The number of RANKL+ cells increased as soon as 12 h, peaked at 18 h and decreased afterwards below baseline values. The increase in RANKL+ cells may be related to the attraction and transit of ED1+ cells from the non-osteogenic compartment to the osteogenic compartment. RANKL "consumption" by the increased pool of migrating precursors and preosteoclasts may cause the subsequent decrease. In contradiction with the current opinion that osteocytes are the main source of RANKL in osteoclastogenesis [8, 34, 35], neighboring osteocytes did not express RANKL. Several observations may explain it: (1) RANKL-expressing osteocytes are associated with the endosteal and endocortical surfaces of the appendicular and axial skeletons [33, 34]; (2) osteoclast-driven tooth eruption is not disturbed by the conditional deletion in osteocytes of the *Tnfsf11* gene that encodes RANKL [34]; (3) contacts between osteoclast precursors and osteocyte dendritic processes are required for RANKL signaling [35], in this model the thickness of the osteogenic compartment prevents such contacts.

Sema3a is primarily a repulsive for sympathetic and sensitive nerve fibers [36, 37]. It also repulses monocytes [38], inhibits osteoclast differentiation upstream RANKL signaling, and is a repellent for osteoclast precursors [26, 39]. In the mandible periosteum osteogenic cells and osteocytes express sema3a [27]. At 24 h the number of sema3a+ cells decreased. This likely relieved the inhibition of osteoclast precursor migration within the osteogenic compartment. Sema3a expression recovery at 48 h may indicate that the number of precursors required
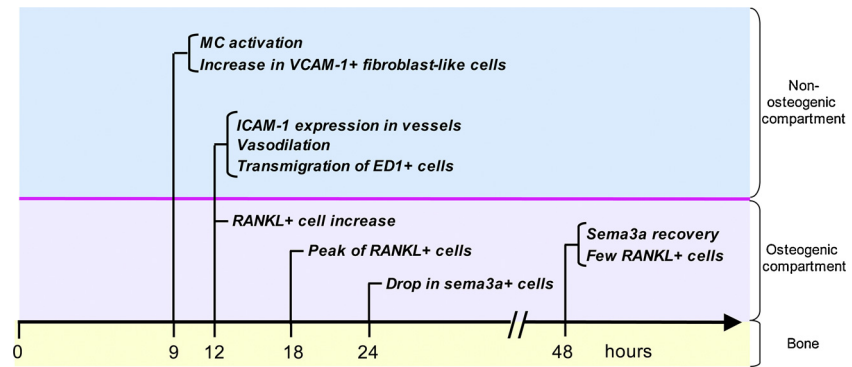
Fig. 5. Diagrammatic representation of the succession of events occurring in the two compartments of the mandible periosteum during activation. The first perceived event is activation of the mast cells close to the vessels in the non-osteogenic compartment. It was followed by vascular reactions and transmigration of inflammatory cells. Simultaneously, an early increase in RANKL expression occurred in the osteogenic compartment. From this moment on, all the events related to osteoclast differentiation and resorption setting, occurred in the osteogenic compartment whilst the non-osteogenic compartment was no longer involved and recovered its basal state. The pink line separates the two compartments.

for resorption had been recruited in the compartment and that inhibition was restored. In fact a fixed number of osteoclast precursors invades the osteogenic compartment during activation [16]; this number was possibly reached at 48 h.

From this study, it is not possible to determine how activation is initially triggered. Changes in mechanical loading in the mandible after maxilla teeth extraction likely induce the release of pro-resorption signals by the osteogenic cells and/or the osteocytes. MC histamine appears to have a central role in the recruitment and possibly guidance of the precursors towards the osteogenic compartment, as its inactivation inhibits the sequence [15, 19]. Since MC form a functional unit with sensory nerves [40], the nervous system may relay the triggering signals to the non-osteogenic compartment via the efferent sympathetic system and the afferent sensory system. Indeed, in this model, sympathectomy [41] and inactivation of the sensory system [42] strongly affect osteoclast precursor recruitment and resorption.

In conclusion, a coordinated sequence of events allowed the recruitment and migration of osteoclast precursors to the mandible cortical bone surface (Fig. 5). This sequence involved the two compartments of the mandible periosteum and several cell types.

Declarations

Author contribution statement

Bassam Hassan, Isabelle Fouilloux: Performed the experiments; Analyzed and interpreted the data.

Brigitte Baroukh: Performed the experiments; Contributed reagents, materials, analysis tools or data.

Annie Llorens: Contributed reagents, materials, analysis tools or data.

Martin Biosse Duplan, Marjolaine Gosset, Marc Cherruau: Conceived and designed the experiments; Wrote the paper.

Jean-Louis Saffar: Conceived and designed the experiments; Analyzed and interpreted the data; Wrote the paper.

Funding statement

Competing interest statement

The authors declare no conflict of interest.

Additional information

No additional information is available for this paper.

References

[1] H.M. Frost, Bone biodynamics, Little, Brown and Company, Boston, 1964.

[2] R. Baron, Importance of the intermediate phases between resorption and formation in the measurement and understanding of the bone remodeling sequence, Bone Histomorphometry. Second Workshop, PJ Meunier edition, Armour-Montagu, Paris, 1977, pp. 179–183.

[3] N.A. Sims, J.H. Gooi, Bone remodeling: Multiple cellular interactions required for coupling of bone formation and resorption, Semin. Cell Dev. Biol. 19 (2008) 444–451.

[4] J.A. Siddiqui, N.C. Partridge, Physiological bone remodeling: Systemic regulation and growth factor involvement, Physiology 31 (2016) 233–245.

[5] W. Xiao, Y. Wang, S. Pacios, S. Li, D.T. Graves, Cellular and molecular aspects of bone remodeling, Front. Oral Biol. 18 (2016) 9–16.

[6] A.M. Parfitt, Osteonal and hemi-osteonal remodeling: the spatial and temporal framework for signal traffic in adult human bone, J. Cell Biochem. 55 (1994) 273–286.

[7] G.A. Rodan, T.J. Martin, Role of osteoblasts in hormonal control of bone resorption. A hypothesis, Calcif. Tissue Int. 33 (1981) 349–351.

[8] T. Bellido, Osteocyte-driven bone remodeling, Calcif. Tissue Int. 94 (2014) 25–34.

[9] N.W.A. McGowan, E.J. Walker, H. MacPherson, S.H. Ralston, M.H. Helfrich, Cytokine-activated endothelium recruits osteoclast precursors, Endocrinology 142 (2001) 1678–1681.

[10] M.L. Brandi, P. Collin-Osdoby, Vascular biology and the skeleton, J. Bone Miner. Res. 21 (2006) 183–192.

[11] P. Collin-Osdoby, L. Rothe, F. Anderson, M. Nelson, W. Maloney, P. Osdoby, Receptor activator of NF-kappa B and osteoprotegerin expression by human microvascular endothelial cells, regulation by inflammatory cytokines, and role in human osteoclastogenesis, J. Biol. Chem. 276 (2001) 20659- –20672.

[12] Y. Tokukoda, S. Takata, H. Kaji, R. Kitazawa, T. Sugimoto, K. Chihara, Interleukin-1 stimulates transendothelial mobilization of human peripheral blood mononuclear cells with a potential to differentiate into osteoclasts in the presence of osteoblasts, Endocr. J. 48 (2001) 443–452.

[13] L. Kindle, L. Rothe, M. Kriss, P. Osdoby, P. Collin-Osdoby, Human microvascular endothelial cell activation by IL-1 and TNF-alpha stimulates the adhesion and transendothelial migration of circulating human CD14+ monocytes that develop with RANKL into functional osteoclasts, J. Bone Miner. Res. 21 (2006) 193–206.

[14] M. Cherruau, F.O. Morvan, A. Schirar, J.L. Saffar, Chemical sympathecto- my-induced changes in TH-, VIP-, and CGRP-immunoreactive fibers in the rat mandible periosteum: influence on bone resorption, J. Cell Physiol. 194 (2003) 341–348.

[15] I. Fouilloux, M. Biosse Duplan, B. Baroukh, M. Cherruau, J.L. Saffar, P. Lesclous, Mast cell activation and degranulation occur early during induction of periosteal bone resorption, Bone 38 (2006) 59–66.

[16] B. Baroukh, M. Cherruau, C. Dobigny, D. Guez, J.L. Saffar, Osteoclasts differentiate from resident precursors in an in vivo model of synchronized resorption: A temporal and spatial study in rats, Bone 27 (2000) 627–634.

[17] T.L. Andersen, T.E. Sondergaard, K.E. Skorzynska, F. Dagnaes-Hansen, T.L. Plesner, E.M. Hauge, T. Plesner, J.M. Delaisse, A physical mechanism for coupling bone resorption and formation in adult human bone, Am. J. Pathol. 174 (2009) 239–247.

[18] M.R. Allen, J.M. Hock, D.B. Burr, Periosteum: biology, regulation, and response to osteoporosis therapies, Bone 35 (2004) 1003–1012.

[19] M. Biosse-Duplan, B. Baroukh, M. Dy, M.C. de Vernejoul, J.L. Saffar, Histamine promotes osteoclastogenesis through the differential expression of histamine receptors on osteoclasts and osteoblasts, Am. J. Pathol. 174 (2009) 1426–1434.

[20] M.W. Greaves, R.A. Sabroe, Histamine the quintessential mediator, J. Dermatol. (1996) 40.

[21] L. Atwood, C. James, G.P. Morris, S. Vanner, Cellular pathways of mast cell and capsaicin-sensitive nerve-evoked ileal submucosal arteriolar dilations, Am. J. Physiol. 275 (1998) G1063–1072.

[22] M. Molla, M. Gironella, R. Miquel, V. Tovar, P. Engel, A. Biete, J.M. Pique, J. Panes, Relative roles of ICAM-1 and VCAM-1 in the pathogenesis of experimental radiation-induced intestinal inflammation, Int. J. Radiat. Oncol. Biol. Phys. 57 (2003) 264–673.

[23] S. Kimura, K.Y. Wang, A. Tanimoto, Y. Murata, Y. Nakashima, Y. Sasaguri, Acute inflammatory reactions caused by histamine via monocytes/macrophages chronically participate in the initiation and progression of atherosclerosis, Pathol. Int. 54 (2004) 465–474.

[24] D. Feuerbach, J.H.M. Feyen, Expression of the cell-adhesion molecule VCAM-1 by stromal cells is necessary for osteoclastogenesis, FEBS Lett 402 (1997) 21–24.

[25] M. Hayashi, T. Nakashima, M. Taniguchi, T. Kodama, A. Kumanogoh, H. Takayanagi, Osteoprotection by semaphorin 3A, Nature 485 (2012) 69–74.

[26] C. Mauprivez, C. Bataille, B. Baroukh, A. Llorens, J. Lesieur, P.J. Marie, J.L. Saffar, M. Biosse Duplan, M. Cherruau, Periosteum metabolism and nerve fiber positioning depend on interactions between osteoblasts and peripheral innervation in rat mandible, Plos One 10 (2015) e0140848.

[27] P.R. Wheather, H.G. Burkitt, V.G. Daniels, P.J. Deakin, Functional histology. A text and colour atlas, 2nd Edition, Churchill Livingstone, Edinburgh, 1987.

[28] A.M. Parfitt, Osteoclast precursors as leukocytes: Importance of the area code, Bone 23 (1998) 491–494.

[29] H. Yusuf-Makagiansar, M.E. Anderson, T.V. Yakovleva, J.S. Murray, T.J. Siahaan, Inhibition of LFA-1/ICAM-1 and VLA-4/VCAM-1 as a therapeutic approach to inflammation and autoimmune diseases, Med. Res. Rev. 22 (2002) 146–167.

[30] J.F. Liu, S.M. Hou, C.H. Tsai, C.Y. Huang, C.J. Hsu, C.H. Tang, CCN4 induces vascular cell adhesion molecule-1 expression in human synovial

fibroblasts and promotes monocyte adhesion, Biochim. Biophys. Acta 1833 (2013) 966–975.

[31] L. Petecchia, L. Serpero, M. Silvestri, F. Sabatini, L. Scarso, G.A. Rossi, The histamine-induced enhanced expression of vascular cell adhesion molecule-1 by nasal polyp-derived fibroblasts is inhibited by levocetirizine, Am. J. Rhinol. 20 (2006) 445–449.

[32] L. Rifas, S.L. Cheng, IL-13 regulates vascular cell adhesion molecule-1 expression in human osteoblasts, J. Cell Biochem. 89 (2003) 213–219.

[33] C.A. O'Brien, T. Nakashima, H. Takayanagi, Osteocyte control of osteoclastogenesis, Bone 5 (2013) 258–263.

[34] J. Xiong, M. Piemontese, M. Onal, J. Campbell, J.J. Goellner, V. Dusevich, L. Bonewald, S.C. Manolagas, C.A. O'Brien, Osteocytes, not osteoblasts or lining cells, are the main source of the RANKL required for osteoclast formation in remodeling bone, Plos One 10 (2015) e0138189.

[35] M. Honma, Y. Ikebuchi, Y. Kariya, M. Hayashi, N. Hayashi, S. Aoki, H. Suzuki, RANKL subcellular trafficking and regulatory mechanisms in osteocytes, J. Bone Miner. Res. 28 (2013) 1936–1949.

[36] M. Taniguchi, S. Yuasa, H. Fujisawa, I. Naruse, S. Saga, M. Mishina, T. Yagi, Disruption of *Semaphorin III/D* gene causes severe abnormality in peripheral nerve projection, Neuron 19 (1997) 519–530.

[37] I. Gavazzi, Semaphorin-neuropilin-1 interactions in plasticity and regeneration of adult neurons, Cell Tissue Res. 305 (2001) 275–284.

[38] S. Delaire, C. Billard, R. Tordjman, A. Chedotal, A. Elhabazi, A. Bensussan, L. Boumsell, Biological activity of soluble CD100. II. Soluble CD100, similarly to H-SemaIII, inhibits immune cell migration, J. Immunol. 166 (2001) 4348–4354.

[39] S. Kang, A. Kumanogoh, Semaphorins in bone development, homeostasis, and disease, Semin. Cell Dev. Biol. 24 (2013) 163–171.

[40] P. Forsythe, J. Bienenstock, The mast cell-nerve functional unit: a key component of physiologic and pathophysiologic responses, Chem. Immunol. Allergy 98 (2012) 196–221.

[41] M. Cherruau, P. Facchinetti, B. Baroukh, J.L. Saffar, Chemical sympathectomy impairs bone resorption in rats: A role for the sympathetic system on bone metabolism, Bone 25 (1999) 545–551.

[42] C. Adam, A. Llorens, B. Baroukh, M. Cherruau, J.L. Saffar, Effects of capsaicin-induced sensory denervation on osteoclastic resorption in adult rats, Exp. Physiol. 85 (2000) 61–66.